# Novel Dielectric-Modulated Field-Effect Transistor for Label-Free DNA Detection

### Chang-Hoon Kim<sup>1</sup>, Cheulhee Jung<sup>2</sup>, Hyun Gyu Park<sup>2</sup> & Yang-Kyu Choi<sup>1</sup>

<sup>1</sup>Division of Electrical Engineering, School of Electrical Engineering and Computer Science, Korea Advanced Institute of Science and Technology (KAIST), Daejeon 305-701, Republic of Korea <sup>2</sup>Department of Chemical and Biomolecular Engineering, Korea Advanced Institute of Science and Technology (KAIST), Daejeon 305-701, Republic of Korea

Correspondence and requests for materials should be addressed to Y.K. Choi (ykchoi@ee.kaist.ac.kr)

Accepted 18 April 2008

#### **Abstract**

This paper describes two competing factors, a dielectric constant and a charge in a dielectric-modulated field-effect transistor (DMFET), for label-free DNA electrical detection. Essentially, the DMFET electrically detects biomolecules by monitoring a change of threshold voltage caused by a change of dielectric constant when targeted biomolecules are confined to a nanogap of the DMFET. In particular, when charged biomolecules such as DNA are introduced into the nanogap, the DMFET operation can be changed by both the dielectric constant and the strength of the charges in the gate dielectric layer.

In this work, negatively-charged DNA and neutralized DNA by sodium ion treatment are carefully compared using an n-channel DMFET in order to verify the contribution to a change of threshold voltage by the DNA charges. In the case of neutralized DNA, the threshold voltage is shifted to the negative side as previously reported. However, in the case of negatively- charged DNA, the threshold voltage is shifted to the positive side due to the negative charges of this DNA. Hence, a p-channel DMFET is clearly preferable in detections of negatively-charged DNA.

**Keywords:** DMFET, DNA, Charge effect, Dielectric constant effect, Label-free electrical detection, Nanogap

#### Introduction

Technical advancements in silicon-based microelectronics have been achieved over the past three de-

cades, primarily through the scaling of device dimensions, in order to attain improvements in circuit speed and a reduction in size according to Moore's law. An essential aspect of this progress is miniaturization using microfabrication technologies<sup>1-3</sup>. Applying silicon microfabrication technology to the detection of nucleic acid hybridization can provide direct electronic detections of biomolecular binding processes. The time and cost of the detection process can be reduced considerably due to a full compatibility with the fabrication process of the semiconductor industry. Nucleic acid hybridization is a rudimentary tool in sequence analysis, gene expression monitoring, genotyping in the fields of genomics and clinical diagnostics, pharmacology, environmental studies, the food industry, and in DNA computing. Thus, various techniques such as fluorescent<sup>4-6</sup>, electrochemical<sup>7-9</sup>, enzymatic<sup>10-11</sup>, and magnetic<sup>12-13</sup> methods have been developed to detect the hybridization of DNA. Unfortunately, these methods require labeling steps, which are unwieldy and time-consuming procedures. As a result, label-free hybridization 14-15 technology has become attractive to researchers in this field. This study reports on a novel approach for label-free detection of DNA hybridization involving the utilization of a nanogap.

Recently, a dielectric-modulated field-effect transistor (DMFET) that had been revamped from a traditional and conventional metal oxide semiconductor field effect transistor (MOSFET) was reported<sup>16</sup>. The DMFET detects biomolecules through change in dielectric constant caused by the introduction of biomolecules in a nanogap located at the edge of the gate dielectric in the DMFET. The as-reported DMFET showed high detection sensitivity for biotin-streptavidin-specific binding, which was known to be nearly neutralized. However, in nature, there are many biomolecules that show charged behaviors; DNA is one of the most important of these biomolecules, as it is known be the largest negatively-charged molecule<sup>17</sup>. When charged biomolecules such as DNA are introduced into the nanogap of a DMFET, its operation can be affected by this charge effect despite the known dielectric constant effect<sup>16</sup>. This study focuses primarily on analyses of these two impacts on labelfree electrical DNA detections. Thus, negativelycharged DNA and neutralized DNA are detected using an n-channel DMFET and are then carefully

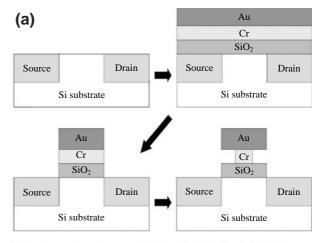
compared. The charge effect is then extracted. It was found that the n-channel DMFET can preferably detect neutralized or positively-charged biomolecules. In contrast, a p-channel DMFET is attractive for improvements to the detection sensitivity of negatively-charged biomolecules.

#### **Results and Discussion**

#### **Device Structure and Fabrication Process**

Figure 1(a) shows a cross-sectional view of a DM-FET. The main difference between a DMFET and a conventional MOSFET involves the nanogap at the edge of the gate dielectric at which biomolecules are attached. In a conventional MOSFET, an applied gate voltage creates an electric field that can affect the channel potential in a silicon substrate through the gate dielectric material. The conventional MOSFET turns on when a channel forms on the silicon substrate by the critical gate voltage, the threshold voltage  $(V_T)$ . In a DMFET, however, the same amount of gate voltage cannot create a great enough electric field that sufficiently turns on the silicon channel because the electric field becomes weakened by the nanogap as it is filled with air. In such a case, the dielectric constant of SiO<sub>2</sub> is 3.9, while that of air is 1. As a result, the  $V_T$  value of the DMFET is larger than that of the conventional MOSFET. However, if the nanogap is filled with biomolecules, the electric field due to the increased dielectric constant, compared to air, is strengthened again; hence,  $V_T$  is decreased. By monitoring this  $V_T$  change, the specific binding of biomolecules can be detected electrically without labeling.

Figure 1(a) shows the fabrication process flow of a DMFET. This process flow is similar to that of a conventional MOSFET. First, source and drain regions are defined by photolithography and ion implantation after a device-isolation step. Subsequently, SiO<sub>2</sub>, Cr, and Au are sequentially grown and deposited by thin film processes. The SiO<sub>2</sub> layer forms the gate dielectric of the DMFET. The Cr layer is a sacrificial layer that leaves the nanogap at the edge of the gate after selective wet etching. The Au layer is the gate electrode of the DMFET. After deposition of these three layers, they are patterned by photolithography and subsequent etching processes. The nanogap was then formed by lateral wet etching of Cr. Figure 1(b) shows a transmission electron microscopy (TEM) image of a cross-sectional view of the nanogap. The height of the nanogap, which was fitted to the size of target molecules, is 15 nm.



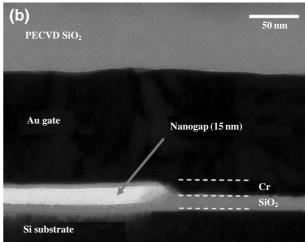


**Figure 1.** (a) process flow and (b) TEM image of the nanogap.

#### Operational Principle and Simulations

In a conventional n-channel MOSFET,  $V_T$ , which determines the on-/off-state of a device, is modeled by Eq. (1).

$$V_T = V_{FB} + 2\varphi_B + \frac{Q_{dep}}{C_{ox}} - \frac{Q_{fix}}{C_{ox}},$$
 (1)

where  $V_T$  is the threshold voltage,  $V_{FB}$  is the flat band voltage,  $\varphi_B$  is the surface-band banding,  $Q_{dep}$  is the depletion charge density in the silicon substrate,  $Q_{fix}$  is the fixed charge density in the SiO<sub>2</sub>, and  $C_{ox}$  is the capacitance of the gate dielectric material (SiO<sub>2</sub>).

By applying this equation to the structure of a DM-FET,  $V_T$  in the nanogap region of the DMFET can be modified by Eqs. (2) and (3).

$$V_T = V_{FB} + 2\varphi_B + \frac{Q_{dep}}{C_{DMFET}} - \frac{Q_{fix}}{C_{DMFET}} \quad \text{and}$$
 (2)

$$\frac{1}{C_{DMFET}} = \frac{1}{C_{mole}} + \frac{1}{C_{air}} + \frac{1}{C_{ox}}$$

$$= \frac{T_{mole}}{k_{mole}\varepsilon_o} + \frac{T_{air}}{\varepsilon_o} + \frac{T_{ox}}{k_{ox}\varepsilon_o},$$
(3)

where  $C_{DMFET}$  is the total capacitance of the gate dielectric materials in the DMFET,  $C_{mole}$ ,  $C_{air}$ , and  $C_{ox}$  indicate the capacitances of the biomolecule, air, and silicon oxide, respectively,  $T_{mole}$ ,  $T_{air}$ , and  $T_{ox}$  denote the thicknesses of the biomolecule, air, and silicon dioxide, respectively, and  $k_{mole}$  and  $k_{ox}$  are the matching dielectric constants of the biomolecule and silicon dioxide, respectively.

In Eq. (2),  $V_{FB}$ ,  $\varphi_B$ , and  $Q_{dep}$  are independent of  $C_{DMFET}$ , which can be changed only by the dielectric constant of the biomolecules and charges ( $Q_{fix}$ ) that the biomolecules have. Apart from the nanogap region in Figure 1(a), silicon dioxide (SiO<sub>2</sub>,  $k_{ox}$ =3.9) is the only dielectric material, and  $V_T$  is always lower in SiO<sub>2</sub> than in the air ( $k_{air}$ =1) nanogap region. Thus,  $V_T$  more sensitively responds to the changes in the diele-

ctric constant in the nanogap region.

In the case of a neutralized DNA introduced in the nanogap,  $V_T$  can be estimated according to Eqs. (2) and (3), and can be changed by the hybridization of a target DNA to a probe DNA previously immobilized in the nanogap. The thickness of the biomolecule layer is fixed; its density begins to increase, which leads an increment of the dielectric constant of the biomolecule layer. Hence, the  $V_T$  shift can be estimated by Eq. (4).

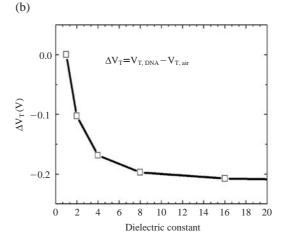
$$\Delta V_T \propto \frac{1}{C_{DMFET}} \propto \frac{1}{k_{mole}} \tag{4}$$

Equation (4) indicates that  $V_T$  decreases when the target DNA attaches. This result was verified by simulation with the aid of SILVACO<sup>18</sup>. Figure 2(a) shows the simulation condition, and Figure 2(b) shows the result of the simulation and a trend that is consistent with Eq. (4).

 $V_T$  can be calculated from Eqs. (2) and (3) when the negatively charged DNA is introduced into the nano-

(a)

Simulation condition		
SiO <sub>2</sub> thickness (T <sub>ox</sub> )	15 nm	
Air gap thickness (Tair)	15 nm	
Substrate doping (N-type)	$10^{15}$ #/cm <sup>3</sup>	
DNA thickness (T <sub>DNA</sub> )	6 nm	
Charge density in air gap	0#/cm <sup>2</sup>	
DNA dielectric constant	1-64	



(c)

Simulation condition	
SiO <sub>2</sub> thickness (T <sub>ox</sub> )	15 nm
Air gap thickness (Tair)	15 nm
Substrate doping (N-type)	$10^{15}$ #/cm <sup>3</sup>
DNA thickness (T <sub>DNA</sub> )	6 nm
Charge density in air gap	0-10 <sup>11</sup> #/cm <sup>2</sup>
DNA dielectric constant	1

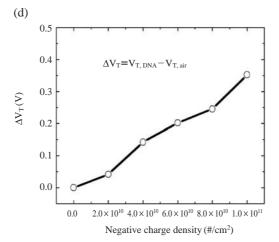


**Figure 2.** Simulation conditions and results: neutralized DNA (a), (b) and negatively-charged DNA (c), (d).

gap. If the dielectric constant change is assumed to be negligible for simplification, the charge density ( $Q_{fix}$ ) due to the target DNA is the only factor that changes  $V_T$ . Subsequently, the  $V_T$  shift can be estimated by Eq. (5).

$$\Delta V_T \propto -Q_{fix} \tag{5}$$

Equation (5) implies that  $V_T$  increases linearly with the hybridized target DNA due to the negative charges of the DNA. This result was also verified by simulation. Figure 2(c) shows the simulation condition while Figure 2(d) shows the results of the simulation and trend that are consistent with Eq. (5).

According to the aforementioned trends of the  $V_T$  shift that were shown to depend on the dielectric constant and charge effect, these two factors can be considered to compete toward an increase or decrease in  $V_T$ . Thus, combining the two factors, a net  $V_T$  shift can be estimated by Eq. (6).

$$\Delta V_T \propto \frac{1}{k_{mole}} (Q_{dep} - Q_{fix}) \tag{6}$$

In order to investigate the trend of  $V_T$  shift for charged biomolecules, another simulation was carried out. Figure 3 shows that  $V_T$  decreases when the dielectric constant of the biomolecule layer is less than 4, whereas it increases when the dielectric constant of the biomolecule layer is larger than 4. In the first region, where  $V_T$  decreases, the dielectric constant effect is dominant. In the second region, where  $V_T$  increases, the charge effect is dominant. Figure 3 also implies that the  $V_T$  shift is not as large as we expected owing to the two competing factors for the negatively-charged DNA detections using the n-channel DMFET.

# The Dielectric Constant Effect Versus the Charge Effect

The first experiment investigated the effect of the dielectric constant versus the charge. Fabricated devices were dipped for 2 hours into a proper solution containing a probe DNA with a SAM layer at one its terminals. One group of samples was then dipped into a neutralized DNA solution for an analysis of the dielectric constant effect, while another group of samples was dipped into a negatively-charged DNA solution for an examination of the charge effect. Additionally, a perfectly-mismatched DNA solution was also used as a third control group.

Figure 4 shows  $V_T$  shifts of the three groups. Figure 4(a) shows the  $V_T$  shift of the perfectly-mismatched DNA, which were not fully hybridized. As expected, there was an insignificant  $V_T$  shift between

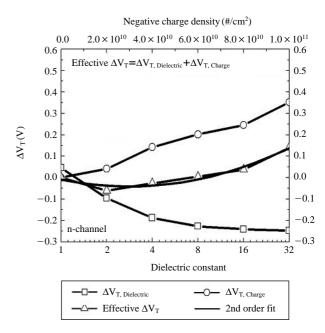


**Figure 3.** Simulation results of an effective threshold voltage shift for both the dielectric constant effect and charge effect.

the immobilization and the hybridization samples. Figure 4(b) shows that the  $V_T$  shift caused by the neutralized DNA that eliminates the charge effect is toward the negative side. This  $V_T$  shift originates from the increment of the dielectric constant in the nanogap due to the increased DNA density. This trend is consistent with theoretical principles, simulation data, and previously reported data<sup>16</sup>. Figure 4(c) shows the  $V_T$  shift caused by the negatively-charged DNA. In contrast, it was shifted to the positive side. In the case of the negatively-charged DNA, the dielectric constant and the charge effect are competing. It can be deduced that the charge effect is more dominant relative to the dielectric constant effect

Figure 4(d) shows comparison data between the neutralized DNA and the negatively-charged DNA. In the neutralized DNA, the  $V_T$  was shifted to the negative side in all four devices that were measured at an average 0.07 V. In the charged DNA, the  $V_T$  was shifted to the positive side in each of the devices, and its average was 0.07 V. From these results, it can be concluded that the dielectric constant effect is dominant in the neutralized DNA and that the charged effect is dominant in the negatively-charged DNA.

#### **True or False Test**

True or false tests were performed in order to confirm that the  $V_T$  shift was caused by the target DNA

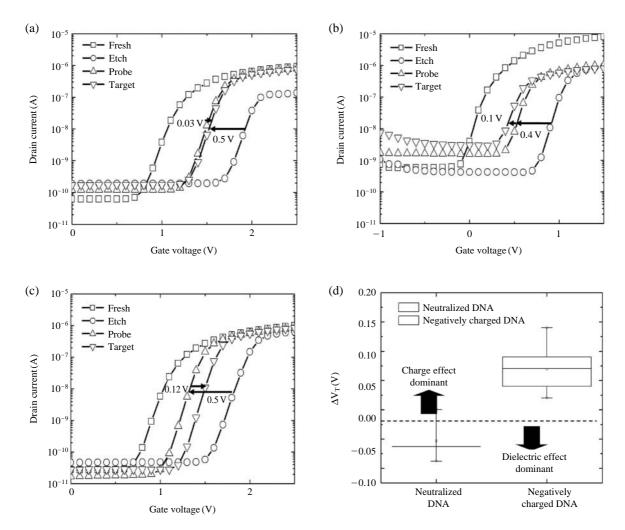


**Figure 4.** The threshold voltage shift by (a) perfectly mismatched DNA, (b) neutralized DNA, (c) negatively-charged DNA, and (d) a comparison of  $V_T$  shift between the neutralized DNA and negatively-charged DNA.

hybridization to the probe DNA. The first experiment compared the  $V_T$  shift between pre-hybridized DNA and sequentially-hybridized DNA. In one control group, a probe DNA was immobilized in the nanogap in a DMFET and a target DNA was then hybridized onto it. In the other control group, a pre-hybridized DNA, hybridized from a probe and a target DNA prior to the introduction to the nanogap, was directly attached to the nanogap. They were compared to the  $V_T$  of a reference sample with no DNA in the nanogap. Figure 5(a) shows that the  $V_T$  shift arises from the introduced DNA in the nanogap.

To ensure that the  $V_T$  shift results from the hybridized DNA, another experiment involving the breaking of the hydrogen bonds in the DNA was carried out. In this experiment, one group contained a probe DNA that was immobilized in the nanogap, while the other group contained a probe DNA and a target

DNA that were sequentially attached and hybridized in the nanogap. These samples were then dipped in hot DI water at 70°C for 10 min in order to break the hybridized DNA bonding between the probe DNA and the target DNA. Figure 5(b) shows that the  $V_T$  shift is approximately 0.1 V, and no significant difference can be seen between them. It can be concluded that the  $V_T$  shift was caused by the hybridization.

It is well known that a MOSFET is very sensitive to alkaline mobile ions such as sodium and potassium in sustaining reliable electrical characteristics. In a previous experiment, sodium was used for the neutralization of DNA, and the electrical characteristics of the DMFET used in the experiment were changed. In order to confirm that the  $V_T$  shift results not from the sodium ions but from the hybridization, another control experiment that measured the effect of the buffer solution was carried out. This solution was a

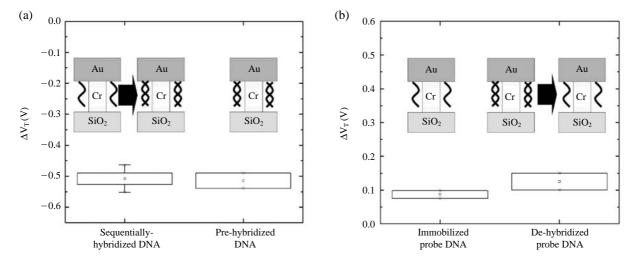


**Figure 5.**  $V_T$  shift of (a) sequentially-hybridized DNA versus pre-hybridized DNA, and (b) an immobilized probe DNA versus a de-hybridized probe DNA by hot DI water.

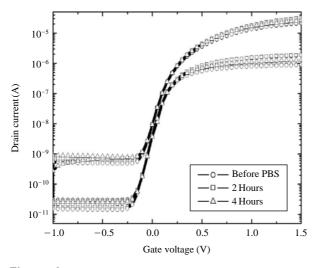


**Figure. 6.** Comparison of transfer characteristics by dipping time in PBS.

phosphate-buffered solution (PBS) that contained many sodium and potassium ions. The DMFETs were dipped in the PBS solution, and the dip time was either 2 hours or 4 hours depending on the samples. The  $V_T$  shifts of the two groups of samples were then measured and compared. Figure 6 shows that the  $V_T$  shift was not affected by the sodium ions in the PBS.

#### **Discussion**

DNA is one of the most important biomolecules in nature, and a DMFET can be one of the most useful

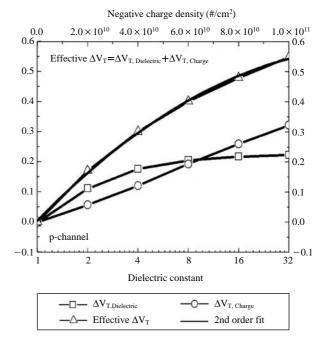


**Figure 7.** Simulation results of effective  $V_T$  shift for both the dielectric constant and the charge effect in a p-channel DMFET.

biosensors to achieve the typical features of biosensors, which can include miniaturization, low-cost fabrication, fast screening, and high sensitivity. Thus, it is timely to realize the feasibility of label-free electrical detections of DNA by DMFETs. It was found that a charge effect occurred in addition to a dielectric constant effect in DMFETs for DNA detection. The

dielectric constant and the charge effect can affect the degree of sensitivity, simultaneously, while acting on the  $V_T$  shift in the opposite manner. The dielectric constant effect shifts  $V_T$  to the negative side, and the charge effect shifts  $V_T$  to the positive side in an nchannel DMFET. As a result, these two effects are offset, and the sensitivity of the DMFET decreases. Although the neutralized DNA can be detected without competition between these two effects, it is less practical. Instead of an n-channel DMFET, a pchannel DMFET is proposed for the detection of negatively-charged biomolecules. Figure 7 shows the simulation results of  $V_T$  shift for a p-channel DM-FET. Both the dielectric constant and the charge effect affect the  $V_T$  shift in the same direction. Therefore, the shift increases, as shown in Figure 7 This implies that the p-channel DMFET guarantees higher sensitivity than the n-channel DMFET for DNA detection. This result also applies to positively-charged biomolecules. Accordingly, with positively-charged biomolecules, the dielectric constant and the charge effect cause the  $V_T$  shift to be moved to the negative side in the n-channel DMFET. Thus, an n-channel or a pchannel DMFET can be chosen according to the charge polarity of targeted biomolecules in order to improve the degree of sensitivity.

# Conclusion

This study reports that a DMFET electrically detected DNA without labeling. When the DNA is neutralized, the threshold voltage decreases due to the dielectric constant effect. In contrast, the threshold voltage increases due to the charge effect when the DNA has negative charges in an n-channel DMFET. Additionally, a p-channel DMFET was proposed so that both the dielectric constant and the charge effect can contribute to changing the threshold voltage in the same direction. This subsequently increases the detection sensitivity.

#### **Materials and Methods**

#### Immobilization and Hybridization of DNA

A DNA sequence composed of 23 nucleotides was extracted from Neisseria Gonorrhoeae DNA. The sequence of a probe DNA that attaches onto the Au surface in the nanogap to hybridize a target DNA is 5'-thiol-TCGAGCATGAACGTCAGTATTAT-3', and the sequence of the target DNA that is detected is 3'-AGCTCGTACTTGCAGTCATAATA-5'. A sequence of DNA not matched to the probe DNA perfectly was

used for a control group; its sequence is 3'-AAGCA-AGTAGTGTTAAAGCGGAA-5'. In the experiment, the probe DNA was attached onto the Au surface of the nanogap, and the target DNA was then hybridized to the probe DNA. In order to attach the probe DNA onto the Au surface, a self-assembly monolayer (SAM) with a thiol- was immobilized at one terminal of the probe DNA. It is well known that the thiol- binds to an Au surface very easily<sup>19</sup>.

DNA has negative charges initially<sup>17</sup>. In order to compare the dielectric constant and the charge effect, neutralized DNA is needed. Neutralized DNA can be obtained by dipping the DNA into a sodium ion solution. In the sodium ion solution, sodium ions combine with phosphoric acid ions on the backbone of the DNA, and the DNA becomes neutralized. In order to confirm the hybridization between the probe DNA and the target DNA, a breaking procedure between them is needed. Ten minutes of dipping in deionized and distilled (DI) water at 70°C is sufficient for this, as the bonds are very week against thermal stimuli<sup>20</sup>.

# **Acknowledgements**

This work was partially supported by the National Research and Development Program (NRDP, 2005-01274) for the development of biomedical function monitoring biosensors, sponsored by the Korea Ministry of Science and Technology (MOST), and the NRL program of KOSEF, grant funded by MOST (No. R0A-2007-000-20028-0).

#### References

- 1. Dennard, R.H. *et al.* Design of ion-implanted MOS-FET's with very small physical dimensions. *IEEE J. Solid-State Circuit* **9**, 256-268 (1974).
- Hu, C. MOSFET scaling in the next decade and beyond. Semiconductor International 105-114 (1994).
- 3. Davari, B. CMOS technology scaling: 0.1 m and beyond. *IEEE International Electron Device Meeting Technical Digest* 555-558 (1996).
- Bras, M. *et al.* Control of immobilization and hybridization on DNA chips by fluorescence spectroscopy. *J. Fluoresc.* 1, 247-253 (2000).
- Marton, M.J. et al. Drug target validation and identification of secondary drug target effects using DNA microarrays. Nat. Med. 4, 1293-1301 (1998).
- 6. Lu, E., Peng, X., Song, F. & Fan, J. A novel fluorescent sensor for triplex DNA. *Bioorg. Med. Chem. Lett.* **15**, 255-257 (2005).
- 7. Palecek, E., Fojta, M., Tomschik, M. & Wang, J. Elec-

- trochemical bisensors for DNA hybridization and DNA damage. *Biosens. Bioelectron.* **13**, 621-628 (1998).
- Marrazza, G., Chianella, I. & Mascini, M. Disposable DNA electrochemical sensor for hybridization detection. *Biosens. Bioelectron.* 14, 43-51 (1999).
- Chen, Y., Elling, Lee, Y.-L. & Chong, S.-C. A fast, sensitive and label free electrochemical DNA sensor. *International MEMS Conference* 204-209 (2006).
- Chen, X. et al. DNA optical sensor: a rapid method for the detection of DNA hybridization. Biosens. Bioelectron 13, 451-458 (1998).
- Defillipo, K.A. & Grayeski, M.L. Flow-injection chemiluminescent method for an enzyme-labelled DNA probe. *Anal. Chim. Acta* 249, 155-162 (1991).
- 12. Miller, M.M. *et al.* A DNA array sensor utilizing magnetic microbeads and magnetoelectronic detection. *J. Magn. Magn. Mater.* **225**, 138-144 (2001).
- 13. Ferreira, H.A. *et al.* Detection of cystic fibrosis related DNA targets using AC field focusing of magnetic labels and spin-valve sensors. *IEEE Trans. Magn.* **41**, 4140-4142 (2005).

- Jang, D.-Y. et al. Sublithographic vertical gold nanogap for label-free electrical detection of protein-ligand binding. J. Vac. Sci. Technol. B 25, 443-447 (2007).
- Peng, H. et al. Label-free electrochemical DNA sensor based on functionalized conducting copolymer. Biosens. Bioelectron 20, 1821-1828 (2005).
- Im, H., Huang, X.-J., Gu, B. & Choi, Y.-K. A dielectric-modulated field-effect transistor for biosensing. Nat. Nanotechnol. 2, 430-434 (2007).
- Kinsella, J.M. & Ivanisevic, A. Taking charge of biomolecules. *Nat. Nanotechnol* 2, 596-597 (2007).
- 18. ATLAS User's Manual. (2000). SILVACO. [Online]. Available: http://www.silvaco.com/products/device\_simulation/atlas.html
- Ohgi, T., Sheng, H.-Y. & Nejoh, H. Au particle deposition onto self-assembled monolayers of thiol and dithiol molecules. *Appl. Surf. Sci.* 130, 919-924 (1998).
- Kondo, S.-I., Sasai, Y. & Kuzuya, M. Development of biomaterial using durable surface wettability fabricated by plasma-assisted immobilization of hydrophilic polymer. *Thin Solid Films* 515, 4136-4140 (2007).